Multiband Material with a Quasi-1D Band as a Robust High-Temperature Superconductor

T. T. Saraiva,[1] P. J. F. Cavalcanti,[2] A. Vagov,[3] A. S. Vasenko,[1,4] A. Perali,[5] L. Dell'Anna,[6] and A. A. Shanenko[1,7,*]

[1]National Research University Higher School of Economics, 101000 Moscow, Russia
[2]Departamento de Fsica, Universidade Federal de Pernambuco, Cidade Universitria, 50670-901 Recife-PE, Brazil
[3]Institut für Theoretische Physik III, Bayreuth Universität, Bayreuth 95440, Germany
[4]Donostia International Physics Center (DIPC), Paseo Manuel de Lardizabal 4, San Sebastián/Donostia, 20018 Basque Country, Spain
[5]School of Pharmacy, Physics Unit, University of Camerino, I-62032 Camerino, Italy
[6]Dipartimento di Fisica e Astronomia "Galileo Galilei," Università di Padova, Via Marzolo 8, 35131 Padova, Italy
[7]Departamento de Fisica, Universidade Federal de Pernambuco, Cidade Universitaria, 50670-901 Recife-PE, Brazil

(Received 27 May 2020; revised 26 August 2020; accepted 26 October 2020; published 18 November 2020)

It is well known that superconductivity in quasi-one-dimensional (Q1D) materials is hindered by large fluctuations of the order parameter. They reduce the critical temperature and can even destroy the superconductivity altogether. Here it is demonstrated that the situation changes dramatically when a Q1D pair condensate is coupled to a higher-dimensional stable one, as in recently discovered multiband Q1D superconductors. The fluctuations are suppressed even by vanishingly small pair-exchange coupling between different band condensates and the superconductor is well described by the mean field theory. In this case the low dimensionality effects enhance the coherence of the system instead of suppressing it. As a result, the critical temperature of the multiband Q1D superconductor can increase by orders of magnitude when the system is tuned to the Lifshitz transition with the Fermi level close to the edge of the Q1D band.

DOI: 10.1103/PhysRevLett.125.217003

It is a common knowledge that superconductivity in 1D systems is suppressed due to large fluctuations of the order parameter. A superconducting state can still be achieved when several 1D structures (parallel chains of molecules or atoms) are coupled one to another, creating a weakly coupled matrix. Earlier theoretical studies demonstrated that such Q1D materials can superconduct [1–4] but the fluctuations are still large, reducing the critical temperature T_c significantly [1]. These predictions were confirmed by the discovery of superconductivity at low temperatures in Bechgaard salts—organic Q1D superconductors [5,6].

Subsequent theoretical efforts have been focused on finding the conditions under which the critical temperature of the Q1D superconductors could be increased rather than reduced. In particular, it was suggested that such an increase can be achieved in the vicinity of the Lifshitz transition at which the chemical potential approaches the edge of the Q1D single-particle energy band [7–11]. However, the fluctuations, that were already very large in the presence of the Q1D effects, are additionally enhanced due to the Bose-like character of the pairing which tends to further deplete the condensate. Enhancement of T_c was found for weakly interacting stripes, formed due to a particular transformation of the antiferromagnetic insulator [12,13]. The effect requires, however, a subtle balance of different interplaying physical mechanisms relevant for superconducting cuprates.

Recently, interest in Q1D superconductors has been boosted by the discovery of Cr_3As_3-chain based materials; see, e.g., Refs. [14–19]. Results of the first principle calculations of the electronic band structure of those compounds led to a conclusion that they are multiband systems, with some of the contributing bands being Q1D [18–20]—multiband Q1D superconductors. For example, $K_2Cr_3As_3$ [19,20] and $KCr_3As_3H_x$ [18] have two Q1D sheets coexisting with one 3D sheet in the Fermi surface. Furthermore, it was demonstrated that in $KCr_3As_3H_x$ the Fermi level can be shifted by changing the H intercalation [18], which gives rise to alterations in topology of the Fermi surface manifested in the Lifshitz transitions.

In this work we show that the advent of multiband Q1D superconductors opens up a fundamental opportunity to achieve superconductivity at high temperatures. It has already been demonstrated that the presence of the pair-exchange coupling between different bands can reduce the fluctuations due to the multiband screening mechanism [21–23]. Motivated by this result as well as by the recent experimental advances, here we investigate a two-band material with coupled Q1D and 3D Bardeen-Cooper-Schrieffer (BCS) condensates, and we demonstrate that under fairly general conditions, it is a robust mean-field superconductor with a critical temperature that can be significantly increased by tuning the Lifshitz transition at the edge of the Q1D band.

We assume s-wave pairing in both the Q1D and 3D bands with Josephson-like interband transfer of Cooper pairs. Superconductivity in this system is described by the standard two-band model introduced in Refs. [24,25].

The intraband and interband pair-exchange couplings are determined by the real matrix $\check{g}$, with the elements $g_{\nu\nu'} = g_{\nu'\nu}$ ($\nu = 1, 2$). For simplicity, we consider the parabolic dispersion of the single-particle energy in both bands. For the same reason, the Fermi surface of the 3D band ($\nu = 1$) is taken spherically symmetric. The principal axis of the Q1D band ($\nu = 2$) is chosen parallel to the z axis. In the x and y directions, the Q1D energy dispersion is degenerate and we assume the effective finite integral of the density of states (DOS) for both these directions. The band-dependent single-particle energies, shifted by the chemical potential μ, are thus given by

$$\xi_{\mathbf{k}}^{(1)} = \varepsilon_0 + \frac{\hbar^2 \mathbf{k}^2}{2m_1} - \mu, \qquad \xi_{\mathbf{k}}^{(2)} = \frac{\hbar^2 k_z^2}{2m_2} - \mu, \tag{1}$$

where $m_{1,2}$ are the effective band masses and $\mathbf{k} = (k_x, k_y, k_z)$. The energy and μ are measured relative to the bottom of the Q1D band. The lowest energy of the 3D band is negative $\varepsilon_0 < 0$ and, to have a BCS-like condensate in the 3D band, we assume $|\varepsilon_0| \gg \mu$. Our study is focused on the superconducting state near the Lifshitz transition at $\mu = 0$. The system is considered in the clean limit, where the role of impurities is neglected. In what follows, we take for the Boltzmann constant $k_B = 1$.

Following Refs. [24,25], the mean-field Hamiltonian of the two-band superconductors is written as

$$\mathcal{H} = \int d^3\mathbf{r} \Bigg\{ \sum_{\nu=1,2} \Bigg[\sum_{\sigma} \hat{\psi}_{\nu\sigma}^{\dagger}(\mathbf{r}) T_{\nu}(\mathbf{r}) \hat{\psi}_{\nu\sigma}(\mathbf{r}) + (\hat{\psi}_{\nu\uparrow}^{\dagger}(\mathbf{r}) \hat{\psi}_{\nu\downarrow}^{\dagger}(\mathbf{r}) \Delta_{\nu}(\mathbf{r}) + \text{H.c.}) \Bigg] + \langle \vec{\Delta}, \check{g}^{-1} \vec{\Delta} \rangle \Bigg\}, \tag{2}$$

where $\hat{\psi}_{\nu\sigma}^{\dagger}(\mathbf{r})$ and $\hat{\psi}_{\nu\sigma}(\mathbf{r})$ are the field operators for the carriers in band ν, $T_{\nu}(\mathbf{r})$ is the single-particle Hamiltonian with the single-particle energies given by Eq. (1), and $\Delta_{\nu}(\mathbf{r})$ is the superconducting gap function for band ν. We also use a vector notation $\vec{\Delta} = (\Delta_1, \Delta_2)$ with $\langle ., . \rangle$ the scalar product in the band vector space, and $\check{g}^{-1}$ is the inverse of the coupling matrix. The band-dependent superconducting gap functions satisfy the self-consistency condition given by the matrix gap equation

$$\vec{\Delta} = \check{g} \vec{R}, \tag{3}$$

where components of $\vec{R}$ are the anomalous Green functions $R_{\nu} = \langle \hat{\psi}_{\nu\uparrow}(\mathbf{r}) \hat{\psi}_{\nu\downarrow}(\mathbf{r}) \rangle$.

The model based on Eqs. (2) and (3) is used to calculate the mean-field critical temperature T_{c0} and then the fluctuation-shifted T_c. T_{c0} is obtained by solving the linearized variant of the gap equation (3). The fluctuations are investigated using the expansion for the free energy functional for the two-band system with respect to the band superconducting gap functions, essentially giving the two-band Ginzburg-Landau (GL) free energy functional.

Assuming that T_{c0} is known, one expands the right-hand side of Eq. (3) with respect to Δ_{ν}. The lowest order terms of this expansion are given by [26–32]

$$R_{\nu}[\Delta_{\nu}] = (\mathcal{A}_{\nu} - a_{\nu}) \Delta_{\nu} - b_{\nu} \Delta_{\nu} |\Delta_{\nu}|^2 + \sum_{i=x,y,z} \mathcal{K}_{\nu}^{(i)} \nabla_i^2 \Delta_{\nu}, \tag{4}$$

where the coefficients $\mathcal{A}_{\nu}$, a_{ν}, b_{ν}, and $\mathcal{K}_{\nu}^{(i)}$ are to be calculated using the microscopic model for each band, and external fields are assumed to be zero.

For the 3D BCS-like band with the spherically symmetric Fermi surface one obtains the standard expressions

$$\mathcal{A}_1 = N_1 \ln\left(\frac{2e^{\gamma}\hbar\omega_c}{\pi T_{c0}}\right), a_1 = -\tau N_1, b_1 = \frac{7\zeta(3)}{8\pi^2}\frac{N_1}{T_{c0}^2},$$
$$\mathcal{K}_1^{(x)} = \mathcal{K}_1^{(y)} = \mathcal{K}_1^{(z)} = \frac{\hbar^2 v_1^2}{6} b_1, \tag{5}$$

where $\tau = 1 - T/T_{c0}$, $\hbar\omega_c$ is the energy cutoff (assumed to be the same for both bands), γ is the Euler constant, $\zeta(x)$ is the Riemann zeta function, the DOS of the 3D band at the Fermi energy is $N_1 = m_1 k_F / 2\pi^2\hbar^2$, and the 3D band Fermi velocity $v_1 = \hbar k_F / m_1$ is determined by the corresponding Fermi wave number $k_F = \sqrt{2m_1(\mu - \varepsilon_0)}/\hbar$.

For the Q1D band the expressions for the coefficients are given by the integrals to be evaluated numerically. At $|\mu| < \hbar\omega_c$ (near the Lifshitz transition) the coefficients can be written as (the derivation is outlined in the Supplemental Material [33]),

$$\mathcal{A}_2 = N_2 \int_{-\tilde{\mu}}^{1} dy \frac{\tanh(y/2\tilde{T}_{c0})}{y\sqrt{y+\tilde{\mu}}},$$
$$a_2 = -\tau \frac{N_2}{2\tilde{T}_{c0}} \int_{-\tilde{\mu}}^{1} dy \frac{\mathrm{sech}^2(y/2\tilde{T}_{c0})}{\sqrt{y+\tilde{\mu}}},$$
$$b_2 = \frac{N_2}{4\hbar^2\omega_c^2} \int_{-\tilde{\mu}}^{1} dy \frac{\mathrm{sech}^2(y/2\tilde{T}_{c0})}{y^3\sqrt{y+\tilde{\mu}}} \left[\sinh\left(\frac{y}{\tilde{T}_{c0}}\right) - \frac{y}{\tilde{T}_{c0}}\right],$$
$$\mathcal{K}_2^{(z)} = \hbar^2 v_2^2 \frac{N_2}{8\hbar^2\omega_c^2} \int_{-\tilde{\mu}}^{1} dy \frac{\sqrt{y+\tilde{\mu}}}{y^3} \mathrm{sech}^2(y/2\tilde{T}_{c0}) \times \left[\sinh\left(\frac{y}{\tilde{T}_{c0}}\right) - \frac{y}{\tilde{T}_{c0}}\right], \qquad \mathcal{K}_2^{(x,y)} = 0, \tag{6}$$

where we use the scaled quantities $\tilde{T}_{c0} = T_{c0}/\hbar\omega_c$ and $\tilde{\mu} = \mu/\hbar\omega_c$, and the effective band velocity v_2 is determined by the cutoff energy as $v_2 = \sqrt{2\hbar\omega_c/m_2}$ (independent of μ). The effective DOS of the Q1D band is given by $N_2 = \sigma_{xy}/4\pi\hbar v_2$, where the factor σ_{xy} accounts for the contribution to the DOS in the x, y dimensions.

The mean-field critical temperature T_{c0} is obtained by solving the linearized gap equation. This reads [see Eqs. (3) and (4)]

$$\check{L}\,\vec{\Delta} = 0, \qquad \check{L} = \check{g}^{-1} - \begin{pmatrix} \mathcal{A}_1 & 0 \\ 0 & \mathcal{A}_2 \end{pmatrix}. \tag{7}$$

This is a matrix equation with solution of the form

$$\vec{\Delta} = \psi(\mathbf{r})\vec{\eta}, \tag{8}$$

where $\vec{\eta}$ is an eigenvector of $\check{L}$ corresponding to its zero eigenvalue, while $\psi(\mathbf{r})$ is a coordinate dependent GL order parameter of the system [31,32]. A nontrivial solution to Eq. (7) exists only when the determinant of $\check{L}$ is zero, which gives the equation

$$(g_{22} - G\mathcal{A}_1)(g_{11} - G\mathcal{A}_2) - g_{12}^2 = 0, \tag{9}$$

with $G = g_{11}g_{22} - g_{12}^2$. Of the two solutions to Eq. (9), one chooses the maximal T_{c0}. The corresponding eigenvector $\vec{\eta}$ can be adopted in the form

$$\vec{\eta} = \begin{pmatrix} S \\ 1 \end{pmatrix}, \qquad S = \frac{g_{11} - G\mathcal{A}_2}{g_{12}}, \tag{10}$$

where S determines the relative weights of the bands, changing from 0 (only band 2) to ∞ (only band 1). We note that the observables are not sensitive to the particular choice of the eigenvector $\vec{\eta}$.

The actual critical temperature T_c is lower than its mean field value T_{c0} due to fluctuations [34]. The fluctuation-induced correction to T_{c0} is obtained by using the standard Gibbs distribution $\exp(-F/T)$, where the free energy functional can be written as (see, e.g., Refs. [27,28])

$$F = \int d^3\mathbf{r}\left[\sum_{\nu=1,2} f_\nu + \langle\vec{\Delta}, \check{L}\,\vec{\Delta}\rangle\right], \tag{11}$$

with

$$f_\nu = a_\nu|\Delta_\nu|^2 + \frac{b_\nu}{2}|\Delta_\nu|^4 + \sum_{i=x,y,z}\mathcal{K}_\nu^{(i)}|\nabla_i\Delta_\nu|^2. \tag{12}$$

The stationary condition for the functional given by Eqs. (11) and (12) yields the gap equation (3).

The calculations of the fluctuation corrections are simplified by representing $\vec{\Delta}$ as a linear combination of the vectors $\vec{\eta}$ and $\vec{\xi} = (1, -S)^T$ [one can see that $\langle\vec{\eta}, \vec{\xi}\rangle = 0$]

$$\vec{\Delta}(\mathbf{r}) = \psi(\mathbf{r})\vec{\eta} + \varphi(\mathbf{r})\vec{\xi}, \tag{13}$$

where $\varphi(\mathbf{r})$ is the second fluctuation mode. The free energy functional is then expressed in terms of ψ and φ as

$$F = \int d^3\mathbf{r}(f_\psi + f_\varphi + f_{\psi\varphi}), \tag{14}$$

where f_ψ and f_φ have the same structure given by Eq. (12), Δ_ν has been replaced by $\psi(\mathbf{r})$ in f_ψ and by $\varphi(\mathbf{r})$ in f_φ, and the set of the coefficients $\{a_\nu, b_\nu, \mathcal{K}_\nu\}$ has been changed to $\{a_\psi, b_\psi, \mathcal{K}_\psi\}$ and $\{\alpha_\varphi, b_\varphi, \mathcal{K}_\varphi\}$. In addition, $f_{\psi\varphi}$ in Eq. (14) represents the coupling between the two modes $\psi(\mathbf{r})$ and $\varphi(\mathbf{r})$. The coefficients in f_ψ one obtained as

$$\begin{aligned} a_\psi &= S^2a_1 + a_2, \qquad b_\psi = S^4b_1 + b_2, \\ \mathcal{K}_\psi^{(i)} &= S^2\mathcal{K}_1^{(i)} + \mathcal{K}_2^{(i)}, \end{aligned} \tag{15}$$

whereas the coefficients in f_φ are given by

$$\begin{aligned} a_\varphi &= a_\varphi^{(0)} + a_1 + S^2a_2, \qquad b_\varphi = b_1 + S^4b_2, \\ \mathcal{K}_\varphi^{(i)} &= \mathcal{K}_1^{(i)} + S^2\mathcal{K}_2^{(i)}, \end{aligned} \tag{16}$$

with

$$a_\varphi^{(0)} = \frac{(1+S^2)^2}{SGg_{12}}. \tag{17}$$

Here $a_\varphi^{(0)} \neq 0$ since S is real. This means that only f_ψ represents the critical fluctuations in the vicinity of the superconducting transition because $a_\psi \to 0$ in the limit $T \to T_{c0}$. The contribution f_φ describes noncritical fluctuations and can be safely omitted [23]. Thus, the fluctuations are determined by the GL functional f_ψ, with the single component order parameter $\psi(\mathbf{r})$. Because of the presence of the Q1D band, this functional is anisotropic with $\mathcal{K}_\psi^{(x,y)} \neq \mathcal{K}_\psi^{(z)}$.

With this simplification, we can apply the known results for the fluctuation-driven shift of the critical temperature in the single-component GL theory. Using the renormalization group approach, one obtains [34] that the actual 3D critical temperature is related to the mean-field temperature by

$$\frac{T_{c0} - T_c}{T_c} = \frac{8}{\pi}\sqrt{\mathrm{Gi}}, \tag{18}$$

where Gi is the Ginzburg number (Ginzburg-Levanyuk parameter). For the 3D anisotropic system this reads [34]

$$\mathrm{Gi} = \frac{1}{32\pi^2}\frac{T_{c0}b_\psi^2}{a_\psi'\mathcal{K}_\psi^{(x)}\mathcal{K}_\psi^{(y)}\mathcal{K}_\psi^{(z)}}, \tag{19}$$

with $a_\psi' = da_\psi/dT$. Using Eq. (15), the above expression can be rearranged as

$$\mathrm{Gi} = \mathrm{Gi}_{3D}\frac{(b_2/b_1 + S^4)^2}{(a_2/a_1 + S^2)(\mathcal{K}_2^{(i)}/\mathcal{K}_1^{(i)} + S^2)S^4}, \tag{20}$$

where Gi_{3D} is the Ginzburg number of the uncoupled (standalone) 3D band, given by Eq. (19) with the

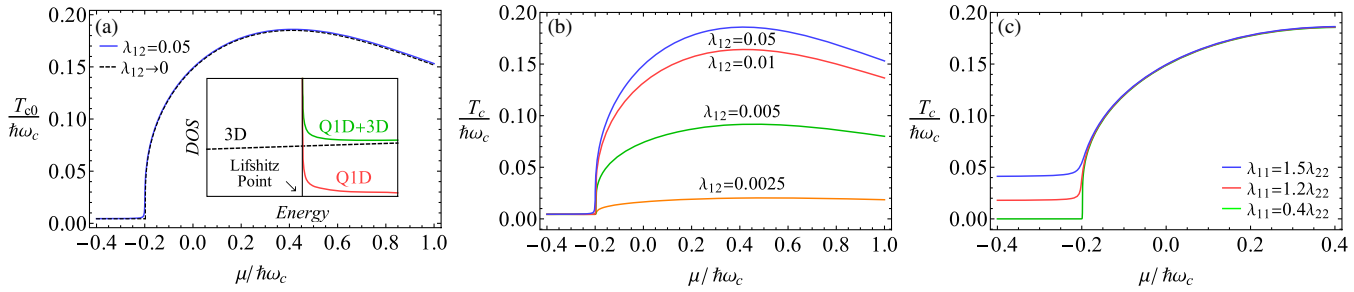

FIG. 1. (a) Mean-field critical temperature T_{c0} versus the chemical potential μ, calculated at $\lambda_{11} = 0.18$, $\lambda_{22} = 0.2$, for $\lambda_{12} = 0.05$ and also for its nearly zero value marked as $\lambda_{12} \to 0$; the inset illustrates the energy dependent DOS for the Q1D and Q1D + 3D systems near the Lifshitz point $E = 0$ (the 3D DOS $\propto \sqrt{E - \varepsilon_0}$ is almost constant near $E = 0$). (b) Fluctuation-shifted critical temperature T_c as a function of μ, calculated for $\lambda_{12} = 0.0025, 0.005, 0.01, 0.05$ at the Ginzburg number of the uncoupled 3D band $\mathrm{Gi}_{3D} = 10^{-10}$; the intraband couplings λ_{11} and λ_{22} are the same as in panel (a). (c) T_c versus μ, calculated for $\lambda_{22} = 0.2$, $\lambda_{11}/\lambda_{22} = 0.4$, 1.2, 1.5, and $\lambda_{12} = 0.05$.

substitution $\{a_\psi, b_\psi, \mathcal{K}_\psi^{(i)}\} \to \{a_1, b_1, \mathcal{K}_1^{(i)}\}$. Equation (20) yields Gi_{3D} in the limit $S \to \infty$ when only the 3D band contributes to the condensate state, and diverges in the opposite limit $S \to 0$ when only the Q1D band contributes, and fluctuations proliferate.

Using Eqs. (9), (18), and (20), we calculate both the mean-field T_{c0} and the fluctuation-shifted T_c. Notice that the multiple microscopic parameters entering these equations reduce to the coupling constants $g_{\nu\nu'}$, band DOS N_ν, and band velocities v_ν. Particle masses m_ν and Q1D DOS factor σ_{xy} are absorbed in those parameters. In addition, $\hbar\omega_c$ sets the energy scale. Below we find it convenient to employ the dimensionless coupling constants $\lambda_{\nu\nu'} = g_{\nu\nu'}\sqrt{N_\nu N_{\nu'}}$.

The number of essential parameters is, actually, even less. S, that determines Gi and T_{c0}, depends only on N_2/N_1 and λ_{ij}. The ratio $\mathcal{K}_2^{(z)}/\mathcal{K}_1^{(z)}$ in Eq. (20) is proportional to v_2^2/v_1^2 and is vanishingly small because v_2 is orders of magnitude less than v_1. N_1 and v_1 are needed to calculate $\mathrm{Gi}_{3D} \simeq (T_{c1,0}/E_F)^4$ (with $T_{c1,0}$ the mean-field critical temperature and $E_F = m_1 v_1^2/2$ the Fermi level of the standalone 3D band). However, we follow a different path and assume $\mathrm{Gi}_{3D} = 10^{-10}$, utilising the fact that Gi lies in the range 10^{-6}–10^{-16} for 3D BCS superconductors [35]. Further, the band-structure calculations for many two-band materials yield $N_2/N_1 \sim 1$, see, e.g., Ref. [36]. Then, as the results depend only weakly on the ratio of the DOSs, we can safely set $N_2/N_1 = 1$. We are left to choose the three remaining parameters λ_{11}, λ_{22}, and λ_{12}.

A typical $T_{c0}(\mu)$ dependence in the vicinity of the Lifshitz transition is shown in Fig. 1(a). In the calculations we utilize $\lambda_{11} = 0.18$ and $\lambda_{22} = 0.2$. However, one can choose any other values in the range typical for conventional superconductors [37]. The pair-exchange coupling is chosen in the interval $0 < \lambda_{12} < 0.05$, keeping in mind that in most multiband superconducting materials λ_{12} is notably smaller than the intraband couplings (see Ref. [36] and references therein).

Figure 1(a) shows that if μ is sufficiently below zero, the Q1D band does not contribute to T_{c0}, and T_{c0} is determined by the 3D band. However, close to $\mu = 0$, T_{c0} increases sharply, approximately by a factor of 40, due to the van Hove singularity at the band edge [see inset in Fig. 1(a)]. The increase starts below the singularity, at $\mu \simeq -0.2$, for which two interconnected factors are responsible: (i) the binding energy of Cooper pairs, estimated as $\max[T_{c0}] \approx 0.2$, and (ii) thermal smoothing of the Fermi surface with nonzero occupation of the Q1D band at $\mu \gtrsim -\max[T_{c0}]$. For large $\mu > \hbar\omega_c$ the contribution of the van Hove singularity vanishes and T_{c0} decreases, following the $1/\sqrt{\mu}$ dependence of the Q1D DOS, and approaches the critical temperature of the 3D band. Figure 1(a) shows that T_{c0} is practically insensitive to the pair-exchange coupling. Consequently, the mean-field characteristics of this two-band superconductor close to the Lifshitz transition are fully determined by the Q1D band.

In contrast, the fluctuation-induced shift of the critical temperature strongly depends on the pair-exchange coupling [Fig. 1(b)]. In the limit $\lambda_{12} \to 0$ the fluctuations suppress the superconductivity. However, this suppression ceases rapidly when λ_{12} increases. Figure 1(b) demonstrates that even a vanishingly small coupling is sufficient to quench the fluctuations and to eliminate the shift. In particular, T_c approaches T_{c0} already by $\lambda_{12} \simeq 0.01$. A generic character of the temperature enhancement and the fluctuations suppression is illustrated in Fig. 1(c), which shows T_c calculated for different values of the ratio $\lambda_{11}/\lambda_{22}$ (at $\lambda_{22} = 0.2$ and $\lambda_{12} = 0.05$). One can see that for $\mu \gtrsim -0.2$ the critical temperature remains nearly the same.

In summary, our analysis demonstrates that the pair-exchange coupling to a stable 3D condensate is capable of quenching severe fluctuations of the Q1D condensate. The suppression mechanism is related to the fact that this coupling creates an anisotropic 3D superconductor with a single critical fluctuation mode, so that Q1D "light" excitations are accompanied by 3D "heavy" excitations, thus reducing the amplitude of the fluctuations.

The stiffness of the critical mode $\mathcal{K}_{\psi}^{(i)}$ is a sum of the band contributions, where the 3D-band contribution dominates as $v_1^2 \gg v_2^2$. We reach the remarkable conclusion that suppression of Q1D fluctuations implies that the two-band system is a robust mean-field superconductor even in the vicinity of the Lifshitz transition.

Although in this work the screening of fluctuations is discussed for s-wave pairing, it is also expected in materials with d-wave symmetry, and even for triplet pairing with a multicomponent order parameter. In this regard, we note that earlier studies of $A_2Cr_3As_3$ (with $A = \mathrm{K, Rb, Sc}$) point to triplet pairing [19,38], although this conclusion is not yet certain [39]. Another class of materials with low-dimensional bands, where a similar multiband mechanism for the fluctuation suppression applies, are organic superconductors such as alkali-metal doped aromatic hydrocarbons [40–44]. The range of achievable T_c's in Fig. 1 can be estimated by considering specific values of the cutoff energy $\hbar\omega_c$. For example, using $\hbar\omega_c \simeq 400$ K, as in Al [37], one gets $\max[T_c] \simeq 70$ K. In organic superconductors $\hbar\omega_c$ can be substantially larger: in K-doped p-terphenyl $K_xC_{18}H_{14}$ the cutoff temperature scale is estimated as $\hbar\omega_c \simeq 1500$ K [11], which yields $\max[T_c] \simeq 250$ K.

We note that the actual increase of T_c can be reduced by various factors, e.g., by smoothing the van Hove singularity due to bending the Q1D Fermi sheet in the direction perpendicular to its principal axis. Another weakening factor is observed in Cr_3As_3-based materials [39], where a strong coupling between distortions of Cr atoms and the 3D Fermi sheet gives rise to a depletion of 3D states thereby reducing screening of the fluctuations. Nevertheless, the enhancement of superconductivity, facilitated by the coupling between a Q1D condensate in the vicinity of the Lifshitz transition and a stable 3D condensate, is a generic phenomenon that leads to a significant amplification of the critical temperature. We note that there are several ways to artificially tune the Lifshitz transition, e.g., by chemical engineering or by doping multiband compounds [18]. Finally, although this work studies the effect of thermal fluctuations on T_c, a similar suppression of quantum fluctuations can be expected at low temperatures near the upper critical field.

A. V. acknowledges the support of the CAPES/Print Grant, Process No. 88887.333666/2019-00 (Brazil). T. T. S. acknowledges financial support and hospitality by the Universities of Camerino and Padova. We thank David Neilson for a critical reading of our manuscript.

*shanenkoa@gmail.com

[1] K. B. Efetov and A. I. Larkin, Effect of fluctuations on the transition temperature in quasi-one-dimensional superconductors, Sov. Phys. JETP **39**, 1129 (1974).

[2] L. P. Gor'kov and I. E. Dzyaloshinskii, Possible phase transitions in systems of interacting metallic filaments (quasiunidimensional metals), Sov. Phys. JETP **40**, 198 (1975).

[3] R. A. Klemm and H. Gutfreund, Order in metallic chains. II. Coupled chains, Phys. Rev. B **14**, 1086 (1976).

[4] H. J. Schulz and C. Bourbonnais, Quantum fluctuations in quasi-one-dimensional superconductors, Phys. Rev. B **27**, 5856 (1983).

[5] D. Jérome, A. Mazaud, M. Ribault, and K. Bechgaard, Superconductivity in a synthetic organic conductor (TMTSF)2PF 6, Phys. Lett. (France) **41**, 95 (1980).

[6] D. Jérome, Historical approach to organic superconductivity, in *The Physics of Organic Superconductors and Conductors*, Springer Series in Materials Science, edited by A. Lebed, Vol. 110, Bollinger Series (Springer, Berlin, 2008).

[7] A. Perali, A. Bianconi, A. Lanzara, and N. L. Saini, The gap amplification at a "shape resonance" in a superlattice of quantum stripes: A mechanism for high T_c, Solid State Commun. **100**, 181 (1996).

[8] A. Bianconi, A. Valletta, A. Perali, and N. L. Saini, High T_c superconductivity in a superlattice of quantum stripes, Solid State Commun. **102**, 369 (1997).

[9] A. A. Shanenko and M. D. Croitoru, Shape resonances in the superconducting order parameter of ultrathin nanowires, Phys. Rev. B **73**, 012510 (2006).

[10] A. A. Shanenko, M. D. Croitoru, A. Vagov, and F. M. Peeters, Giant drop in the Bardeen-Cooper-Schrieffer coherence length induced by quantum size effects in superconducting nanowires, Phys. Rev. B **82**, 104524 (2010).

[11] M. V. Mazziotti, A. Valletta, G. Campi, D. Innocenti, A. Perali, and A. Bianconi, Possible Fano resonance for high-T_c multi-gap superconductivity in p-Terphenyl doped by K at the Lifshitz transition, Europhys. Lett. **118**, 37003 (2017).

[12] S. A. Kivelson, E. Fradkin, and V. J. Emery, Electronic liquid-crystal phases of a doped Mott insulator, Nature (London) **393**, 550 (1998).

[13] E. Arrigoni, E. Fradkin, and S. A. Kivelson, Mechanism of high-temperature superconductivity in a striped Hubbard model, Phys. Rev. B **69**, 214519 (2004).

[14] J.-K Bao, J-Y. Liu, C.-W. Ma, Z.-H. Meng, Z.-T. Tang, Y.-L. Sun, H.-F. Zhai, H. Jiang, H. Bai, C.-M Feng, Z.-A. Xu, and G.-H. Cao, Superconductivity in Quasi-One-Dimensional $K_2Cr_3As_3$ with Significant Electron Correlations, Phys. Rev. X **5**, 011013 (2015).

[15] H. Z. Zhi, T. Imai, F. L. Ning, J.-K. Bao, and G.-H. Cao, NMR Investigation of the Quasi-One-Dimensional Superconductor $K_2Cr_3As_3$, Phys. Rev. Lett. **114**, 147004 (2015).

[16] Z.-T. Tang, J.-K. Bao, Y. Liu, Y.-L. Sun, A. Ablimit, H.-F. Zhai, H. Jiang, C.-M. Feng, Z.-A. Xu, and G.-H. Cao, Unconventional superconductivity in quasi-one-dimensional $Rb_2Cr_3As_3$, Phys. Rev. B **91**, 020506(R) (2015).

[17] Z.-T. Tang, J.-K. Bao, Z. Wang, H. Bai, H. Jiang, Y. Liu, H.-F. Zhai, C.-M. Feng, Z.-A. Xu, and G.-H. Cao, Superconductivity in quasi-one-dimensional $Cs_2Cr_3As_3$ with large interchain distance, Sci. China Mater. **58**, 16 (2015).

[18] S.-Q. Wu, C. Cao, and G.-H. Cao, Lifshitz transition and nontrivial H-doping effect in the Cr-based superconductor $KCr_3As_3H_x$, Phys. Rev. B **100**, 155108 (2019).

[19] C. Xu, N. Wu, G. Zhi, B.-H. Lei, Xu Duan, F. Ning, Ch. Cao, and Q. Chen, Coexistence of nontrivial topological properties and strong ferromagnetic fluctuations in

quasi-one-dimensional $A_2Cr_3As_3$, npj Comput. Mater. **6**, 30 (2020).
[20] H. Jiang, G. Cao, and C. Cao, Electronic structure of quasi-one-dimensional superconductor $K_2Cr_3As_3$ from first-principles calculations, Sci. Rep. **5**, 16054 (2015).
[21] A. Perali, C. Castellani, C. Di Castro, M. Grilli, E. Piegari, and A. A. Varlamov, Two-gap model for underdoped cuprate superconductors, Phys. Rev. B **62**, 9295(R) (2000).
[22] S. Wolf, A. Vagov, A. A. Shanenko, V. M. Axt, A. Perali, and J. Albino Aguiar, BCS-BEC crossover induced by a shallow band: Pushing standard superconductivity types apart, Phys. Rev. B **95**, 094521 (2017).
[23] L. Salasnich, A. A. Shanenko, A. Vagov, J. Albino Aguiar, and A. Perali, Screening of pair fluctuations in superconductors with coupled shallow and deep bands: A route to higher-temperature superconductivity, Phys. Rev. B **100**, 064510 (2019).
[24] H. Suhl, B. T. Matthias, and L. R. Walker, Bardeen-Cooper-Schrieffer Theory of Superconductivity in the Case of Overlapping Bands, Phys. Rev. Lett. **3**, 552 (1959).
[25] V. A. Moskalenko, Superconductivity of metals, taking into account the overlapping of energy bands, Phys. Met. Metallogr. **8**, 25 (1959).
[26] B. T. Geilikman, R. O. Zaitsev, and V. Z. Kresin, Properties of superconductors having overlapping bands, Sov. Phys. Solid State **9**, 642 (1967).
[27] I. N. Askerzade, A. Gencer, and N. Güclü, On the Ginzburg-Landau analysis of the upper critical field H_{c2} in MgB_2, Supercond. Sci. Technol. **15**, L13 (2002).
[28] M. E. Zhitomirsky and V.-H. Dao, Ginzburg-Landau theory of vortices in a multigap superconductor, Phys. Rev. B **69**, 054508 (2004).
[29] V. G. Kogan and J. Schmalian, Ginzburg-Landau theory of two-band superconductors: Absence of type-1.5 superconductivity, Phys. Rev. B **83**, 054515 (2011).
[30] A. A. Shanenko, M. V. Milošević, F. M. Peeters, and A. V. Vagov, Extended Ginzburg-Landau Formalism for Two-Band Superconductors, Phys. Rev. Lett. **106**, 047005 (2011).
[31] A. Vagov, A. A. Shanenko, M. V. Milošević, V. M. Axt, and F. M. Peeters, Two-band superconductors: Extended Ginzburg-Landau formalism by a systematic expansion in small deviation from the critical temperature, Phys. Rev. B **86**, 144514 (2012).
[32] N. V. Orlova, A. A. Shanenko, M. V. Milošević, F. M. Peeters, A. V. Vagov, and V. M. Axt, Ginzburg-Landau theory for multiband superconductors: Microscopic derivation, Phys. Rev. B **87**, 134510 (2013).
[33] See Supplemental Material at http://link.aps.org/supplemental/10.1103/PhysRevLett.125.217003 for derivation details for Q1D band.
[34] A. Larkin and A. Varlamov, *Theory of Fluctuations in Superconductors* (Oxford University Press, Oxford, 2005).
[35] J. B. Ketterson and S. N. Song, *Superconductivity* (Cambridge University Press, Cambridge, England, 1999).
[36] A. Vagov, A. A. Shanenko, M. V. Milošević, V. M. Axt, V. M. Vinokur, J. Albino Aguiar, and F. M. Peeters, Superconductivity between standard types: Multiband versus single-band materials, Phys. Rev. B **93**, 174503 (2016).
[37] A. L. Fetter and J. D. Walecka, *Quantum Theory of Many-Particle Systems* (Dover, New York, 2003).
[38] X. Wu, F. Yang, C. Le, H. Fan, and J. Hu, Triplet p_z-wave pairing in quasi-one-dimensional superconductors $A_2Cr_3As_3$ (A = K, Rb, Sc), Phys. Rev. B **92**, 104511 (2015).
[39] G. Xing, L. Shang, Y. Fu, W. Ren, X. Fan, W. Zheng, and D. J. Singh, Structural instability and magnetism of superconducting KCr_3As_3, Phys. Rev. B **99**, 174508 (2019).
[40] R. Mitsuhashi, Y. Suzuki, Y. Yamanari, H. Mitamura, T. Kambe, N. Ikeda, H. Okamoto, A. Fujiwara, M. Yamaji, N. Kawasaki, Y. Maniwa, and Y. Kubozono, Superconductivity in alkali-metal-doped picene, Nature (London) **464**, 76 (2010).
[41] Y. Gao, R.-S. Wang, X.-L. Wu, J. Cheng, T.-G. Deng, X.-W. Yan, and Z.-B. Huang, Searching superconductivity in potassium-doped p-terphenyl, Acta Phys. Sin. **65**, 077402 (2016).
[42] W. Liu, H. Lin, R. Kang, X. Zhu, Y. Zhang, S. Zheng, and H.-H. Wen, Magnetization of potassium-doped p-terphenyl and p-quaterphenyl by high-pressure synthesis, Phys. Rev. B **96**, 224501 (2017).
[43] J.-F. Yan, G.-H. Zhong, R.-S. Wang, K. Zhang, H.-Q. Lin, and X.-J. Chen, Superconductivity and phase stability of potassium-intercalated p-quaterphenyl, J. Phys. Chem. Lett. **10**, 40 (2019).
[44] L. Haoxiang, X. Zhou, S. Parham, T. Nummy, J. Griffith, K. N. Gordon, E. L. Chronister, and D. S. Dessau, Spectroscopic evidence of low-energy gaps persisting up to 120 K in surface-doped *p*-terphenyl crystals, Phys. Rev. B **100**, 064511 (2019).